Thermal Critical Points and Quantum Critical End Point in the Frustrated Bilayer Heisenberg Antiferromagnet

J. Stapmanns,[1] P. Corboz,[2] F. Mila,[3] A. Honecker,[4] B. Normand,[5] and S. Wessel[1]
[1]Institut für Theoretische Festkörperphysik, JARA-FIT and JARA-HPC, RWTH Aachen University, 52056 Aachen, Germany
[2]Institute for Theoretical Physics and Delta Institute for Theoretical Physics, University of Amsterdam, Science Park 904, 1098 XH Amsterdam, Netherlands
[3]Institute of Physics, Ecole Polytechnique Fédérale Lausanne (EPFL), 1015 Lausanne, Switzerland
[4]Laboratoire de Physique Théorique et Modélisation, CNRS UMR 8089, Université de Cergy-Pontoise, 95302 Cergy-Pontoise Cedex, France
[5]Neutrons and Muons Research Division, Paul Scherrer Institute, 5232 Villigen-PSI, Switzerland

(Received 14 June 2018; published 17 September 2018)

We consider the finite-temperature phase diagram of the $S = 1/2$ frustrated Heisenberg bilayer. Although this two-dimensional system may show magnetic order only at zero temperature, we demonstrate the presence of a line of finite-temperature critical points related to the line of first-order transitions between the dimer-singlet and -triplet regimes. We show by high-precision quantum Monte Carlo simulations, which are sign-free in the fully frustrated limit, that this critical point is in the Ising universality class. At zero temperature, the continuous transition between the ordered bilayer and the dimer-singlet state terminates on the first-order line, giving a quantum critical end point, and we use tensor-network calculations to follow the first-order discontinuities in its vicinity.

DOI: 10.1103/PhysRevLett.121.127201

The concept of the critical point is ubiquitous in statistical thermodynamics. One may need look no further than the liquid-gas transition [1] in systems as familiar as water to find examples where a line of first-order transitions terminates as a function of temperature and a control parameter, such as the pressure. Because the phase transitions are discontinuous, the line has no critical properties, but its termination point does. In contrast with this critical point, the term "critical end point" (CEP) is reserved for the situation where a line of continuous transitions terminates on a line of discontinuous ones [2–4]. In this case, critical behavior is present everywhere on the critical line, and it has been proposed that this behavior is reflected in certain properties of the discontinuous boundary on which the line terminates [4].

Quantum spin systems have proven to offer an excellent forum for the experimental and theoretical investigation of phase transitions and critical phenomena. Quantum phase transitions (QPTs) [5], predominantly in low-dimensional systems, have been controlled by pressure [6], applied magnetic field [7,8], and sample disorder [9], and the associated quantum critical regime [5] explored at finite temperatures [10]. Frustrated quantum magnets extend the nature of the available QPTs to include exact ground states [11,12], exotic bound states [13,14], spin liquids [15], and nontrivial topology [16]. Here we consider the frustrated bilayer $S = 1/2$ antiferromagnet, a two-dimensional (2D) model with Heisenberg exchange.

In this Letter we demonstrate that, although this system has long-ranged magnetic order and spontaneous breaking of SU(2) symmetry only at zero temperature, a line of critical points appears at finite temperature, T. As T is increased, each critical point can be understood as the termination of a line of finite-T first-order transitions, exactly like the critical point of the liquid-gas transition, and all have Ising nature. The critical line is associated with a line of first-order transitions at $T = 0$, where we show that the phase diagram as a function of frustration contains a quantum critical end point (QCEP), at which a line of continuous transitions terminates on the line formed by the first-order quantum phase transitions.

We are motivated by our study of the frustrated spin ladder [17], and in particular of its perfectly frustrated limit [13,14]. Like its 1D analog, the frustrated bilayer has a first-order transition between dimer-singlet and -triplet regimes, and in the fully frustrated case it has completely flat excitation bands composed of many-particle bound states. However, in 2D, magnetic order is possible at $T = 0$, on top of which thermal fluctuations may cause qualitatively different physics to set in.

The model we investigate is represented schematically in the insets of Fig. 1. In addition to the interaction, $J_\perp$, defining the dimer unit and the intralayer interaction, $J_\parallel$, defining the two planes of the system, we include a symmetrical, diagonal, and frustrating interlayer coupling, $J_\times$. Only antiferromagnetic couplings are considered. The Hamiltonian for any quantum spin S is

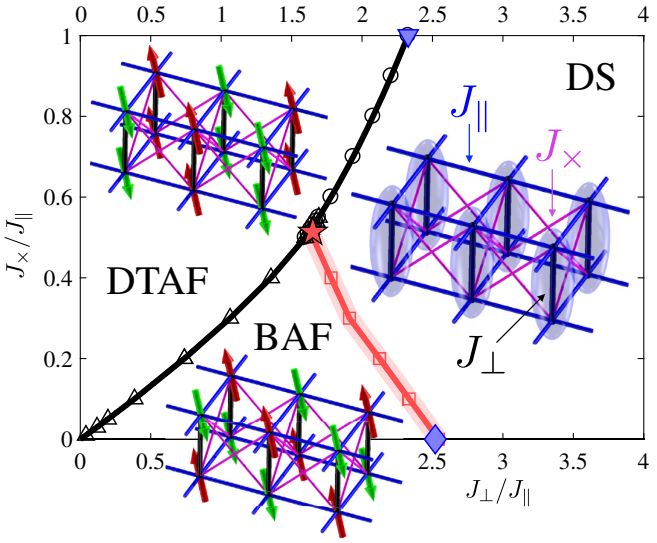

FIG. 1. Phase diagram of the frustrated Heisenberg bilayer at zero temperature. DS: dimer-singlet regime; DTAF: dimer-triplet antiferromagnet; BAF: bilayer antiferromagnet. Insets provide schematic representations of the three phases, where each site hosts an $S = 1/2$ quantum spin, ellipsoids represent singlet states of two spins, and the Heisenberg couplings between spins are specified by the parameters $J_\perp$, $J_\parallel$, and $J_\times$. The line of first-order transitions from DTAF to DS or BAF phases is shown in black and the line of second-order transitions from the DS phase to the BAF phase in red; red shading indicates the error bars in our calculations. Blue symbols denote the QPTs in the unfrustrated (UFB, diamond) and fully frustrated (FFB, triangle) bilayers. The red star denotes the QCEP, where the red line terminates on the black one.

$$H = \sum_i J_\perp \vec{S}_{i,1} \cdot \vec{S}_{i,2} + \sum_{\substack{i,m=1,2 \\ j=i+\hat{x},i+\hat{y}}} [J_\parallel \vec{S}_{i,m} \cdot \vec{S}_{j,m} + J_\times \vec{S}_{i,m} \cdot \vec{S}_{j,\bar{m}}], \tag{1}$$

where i is the dimer bond index, j denotes the nearest-neighbor dimers in the bilayer, $m = 1$ and 2 denote the two layers, and $\bar{m}$ is the layer opposite to m.

Our initial focus is the fully frustrated bilayer (FFB), $J_\times = J_\parallel$. In this situation, Eq. (1) can be reexpressed as

$$H = J_\parallel \sum_{i,j} \vec{T}_i \cdot \vec{T}_j + J_\perp \sum_i \left[\frac{1}{2} \vec{T}_i^2 - S(S+1) \right], \tag{2}$$

where $\vec{T}_i = \vec{S}_{i,1} + \vec{S}_{i,2}$ is the total spin of dimer i [18,19]. Clearly Eq. (2) has one purely local conservation law, on $\vec{T}_i^2$, for every dimer in the system. Henceforth we restrict our considerations to the case $S = 1/2$. Thus T_i takes the values 0 [a dimer singlet (DS), indicated by the ellipsoids in Fig. 1] or 1 [a dimer triplet (DT)]. For a given set $\{T_i\}$, the first term of Eq. (2) is the Hamiltonian of an open n-site spin-1 cluster, which is nonzero only for groups of $n \geq 2$ neighboring DTs; the second term counts these DTs relative to DSs.

As first noted [20] for the fully frustrated $S = 1/2$ ladder, the model of Eq. (2) possesses a first-order DS-to-DT QPT as a function of the coupling ratio $J_\perp/J_\parallel$; the two possible ground states are characterized by all $T_i = 0$, when $J_\perp$ is dominant, or all $T_i = 1$ when the combination of $J_\parallel$ and $J_\times$ forces the creation of DTs. For the FFB, the ground state in the DT phase exhibits long-range antiferromagnetic order of the triplet states, which we denote DTAF. Based on energy arguments comparing the DS state with the spin-1 square-lattice Heisenberg model equivalent to the DTAF state, this transition is known to occur at $J_{\perp,c} = 2.3279(1)J_\parallel$ [21]. Several authors have studied this system, notably by the construction of exact states [22,23] and in a magnetic field [24–26], and its geometry is realized in the material $Ba_2CoSi_2O_6Cl_2$ [27,28], albeit with predominantly XY interactions.

We use stochastic series expansion [29] quantum Monte Carlo (QMC) simulations with directed loop updates [30,31] to examine the thermodynamic properties of the FFB in the vicinity of the QPT. It has been shown recently [13,17,32,33] that QMC methods can be applied to such highly frustrated systems by expressing the Hamiltonian in the dimer basis [Eq. (2)]. The sign problem is entirely absent in perfectly frustrated models, including the FFB, and is only moderately serious over a wide range of coupling ratios corresponding to imperfect frustration, as we show in Sec. S1 of the Supplemental Material [34]. Combined with a parallel tempering approach [13], required to enhance state mixing in the vicinity of the first-order QPT, we access system sizes $2 \times L \times L$ up to $L = 48$ within the temperature regime relevant for the critical point ($T \gtrsim 0.3J_\parallel$). At lower temperatures, strong hysteresis effects appear for couplings close to the QPT.

The thermodynamic properties obtained from QMC simulations for the FFB are shown in Fig. 2. The magnetic susceptibility, $\chi(T)$ [Fig. 2(a)], provides a clear characterization of the gapped DS phase for $J_\perp > J_{\perp,c}$, namely, an exponentially rapid rise to a broad peak, and of the DTAF phase for $J_\perp < J_{\perp,c}$, where χ approaches a finite value at low T; this constant is the same as for the spin-1 Heisenberg model on the square lattice. The first hint of critical-point behavior is provided by the energy [Fig. 2(b)], which shows a clear discontinuity as a function of the coupling ratio at lower temperatures, but a continuous evolution at higher ones. To examine this in more detail we consider the dimer singlet density, $\rho_s = \langle N_s \rangle / N_d$, where N_d is the number of dimer ($J_\perp$) bonds and $N_s = \sum_i P_{s,i}$ the number operator for singlets on these bonds, $P_{s,i}$ being a local singlet projector on bond i; the DT density is simply $\rho_t = 1 - \rho_s$. In the ground state, ρ_s jumps directly from 0 to 1 at $J_{\perp,c}$. We observe [Fig. 2(d)] that this discontinuity persists up to $T \simeq 0.54J_\parallel$, whereas ρ_s varies smoothly across $J_{\perp,c}$ at

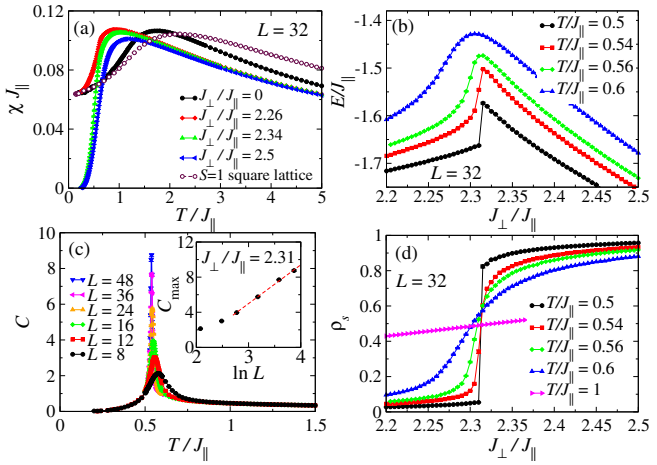

FIG. 2. Thermodynamic properties of the FFB determined from QMC simulations. (a) Magnetic susceptibility, $\chi(T)$, shown for a wide range of coupling ratios. (b) Energy, E, as a function of $J_\perp/J_\parallel$ for different temperatures. (c) Specific heat, $C(T)$, computed at $J_\perp/J_\parallel = 2.31$. Inset: Finite-size scaling of peak height, $C_{\max}$. (d) Singlet density, ρ_s, as a function of $J_\perp/J_\parallel$ for different temperatures.

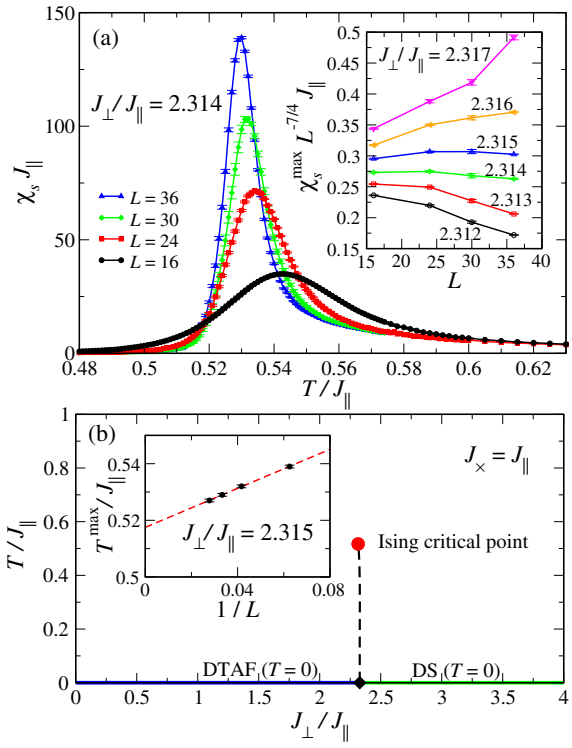

FIG. 3. (a) Singlet susceptibility, $\chi_s(T)$, computed for systems of different sizes, L. Inset: Finite-size scaling of the rescaled peak height for different values of $J_\perp/J_\parallel$. (b) Phase diagram of the FFB. The dashed line marks the finite-temperature first-order transition and the red dot the Ising critical point, $(J_{\perp,I}, T_I) = (2.315(1)J_\parallel, 0.517(3)J_\parallel)$. Blue and green colors represent, respectively, the pure DTAF and DS phases at $T = 0$, where the QPT occurs at $J_{\perp,c} = 2.3279(1)J_\parallel$. Inset: Finite-size scaling of the temperature, $T^{\max}$, of the peak in $\chi_s(T)$ for coupling ratio $J_\perp/J_\parallel = 2.315$.

higher T. Thus although magnetic order is found only in the DTAF at $T = 0$, the transition from predominantly DT to predominantly DS character persists as a first-order line to finite temperatures, of the same order as the interaction parameters, before terminating at an apparent critical point.

To rationalize the appearance of critical-point physics, we note that the singlet and triplet states on each dimer unit form a binary degree of freedom. This effective Ising variable corresponds to the two distinct irreducible representations of the spin in the two-site unit cell ($2 \otimes 2 = 1 \oplus 3$). The line of first-order transitions from DS- to DT-dominated states at finite temperatures may thus terminate at a finite-T Ising critical point, which resembles the liquid-gas transition. This result reflects a key additional property of the SU(2)-symmetric frustrated bilayer model. Although the continuous symmetry precludes a finite order parameter at $T > 0$, thermal fluctuations of the binary variable, whose origin lies in the two-site nature of the unit cell, nevertheless stabilize a critical point.

To identify this Ising critical point in the FFB, we employ finite-size scaling of several thermodynamic quantities. In Fig. 2(c) we show that the specific heat, $C(T)$, computed at $J_\perp \approx J_{\perp,c}$, develops a sharp peak at $T \simeq 0.55J_\parallel$. The logarithmic form [41] of the size-scaling of the peak height ($C_{\max}$, shown in the inset) indicates that the transition we observe is consistent with emerging Ising universality.

Our most accurate means of locating the critical point is to compute the singlet susceptibility, $\chi_s = \beta/N_d(\langle N_s^2\rangle - \langle N_s\rangle^2)$. Figure 3(a) shows that $\chi_s(T)$, computed for a value of $J_\perp/J_\parallel$ very near our final estimate of the critical point and for a number of system sizes, also shows a sharp peak at the same temperature. The inset shows the dependence on L of the peak maximum, $\chi_s^{\max}$, scaled by $L^{7/4}$ [42], where the curve becoming flat (around $J_\perp/J_\parallel = 2.315$) is in accord with 2D Ising universality. At smaller (larger) values of $J_\perp/J_\parallel$, the rescaled $\chi_s^{\max}$ bends downwards (upwards) with increasing L, indicative of subcritical (first-order) behavior.

We draw the coupling-temperature phase diagram of the FFB in Fig. 3(b). Our estimate of the Ising critical point is $(J_{\perp,I}, T_I) = (2.315(1)J_\parallel, 0.517(3)J_\parallel)$, where T_I is based on finite-size scaling of the form $T^{\max}(L) - T_I \propto 1/L^\nu$, with $\nu = 1$ for 2D Ising criticality [43] [inset, Fig. 3(b)]. Although this first-order line appears to be very steep on the scale of Fig. 3(b) ($J_{\perp,c} = 2.3279(1)J_\parallel$ at $T = 0$ [21]), its precise shape is a nontrivial consequence of the interplay between quantum and thermal fluctuations, which we analyze in Sec. S2 of the Supplemental Material [34].

To address the generality of this critical-point phenomenology, we consider the bilayer model away from perfect frustration. We first draw the ground-state phase diagram connecting the FFB to its unfrustrated counterpart (Fig. 1).

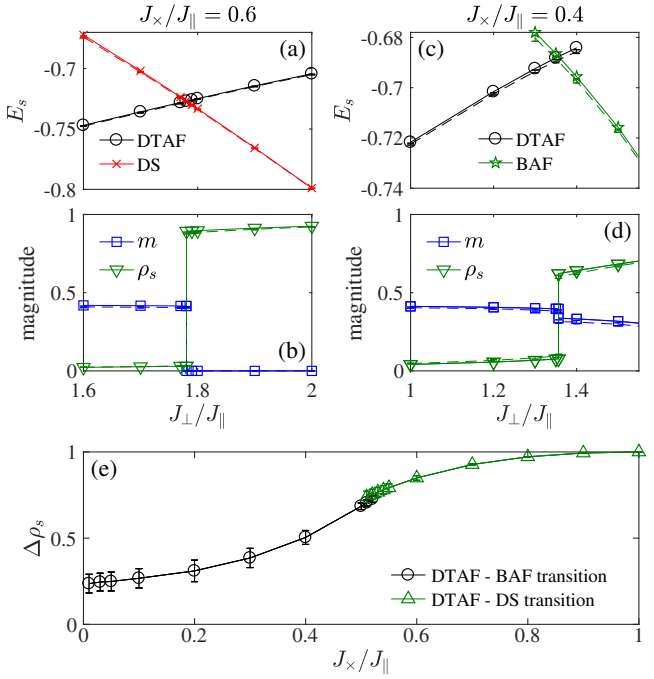

FIG. 4. (a) Energies of the DTAF and DS phases as functions of $J_\perp/J_\parallel$ at $J_\times/J_\parallel = 0.6$; the line-crossing marks the first-order transition. Full lines show (simple-update) iPEPS results with $D = 10$, dashed lines the $D \to \infty$ extrapolated results. (b) Corresponding singlet density, ρ_s, and local magnetic moment, m. (c),(d) As for (a) and (b) with $J_\times/J_\parallel = 0.4$, where the transition is between DTAF and BAF. (e) Discontinuity in ρ_s, taken from data extrapolated in D, shown along the entire first-order transition line of Fig. 1.

The unfrustrated bilayer (UFB) also has two phases at $T = 0$, an ordered $S = 1/2$ bilayer AF (BAF) at small $J_\perp$ and a DS phase otherwise. This model has been studied extensively, including in Refs. [44–48], and the QPT is known to occur at $J_\perp/J_\parallel = 2.5220(2)$ [48]. This transition is second-order, with 3D O(3) universality and continuous growth of the BAF order parameter, which is quite different from that of the DTAF (insets, Fig. 1).

We compute the ground-state phase diagram by the method of infinite projected entangled pair states (iPEPS) [49–51], which is a variational tensor-network ansatz for a 2D wave function in the thermodynamic limit. As we discuss in Sec. S3 of the Supplemental Material [34], the accuracy of this technique can be controlled systematically by the bond dimension, D, of the tensors, and tensor optimization was performed using both the simple- [52,53] and full-update approaches [51,54]. Estimates of energies, singlet densities, and magnetic order parameters in the limit of infinite D were obtained by extrapolation in $1/D$ [55], as illustrated in the Supplemental Material [34]. We show our results in Figs. 4(a) and 4(b) for a constant frustration ratio $J_\times/J_\parallel = 0.6$ and in Figs. 4(c) and 4(d) for $J_\times/J_\parallel = 0.4$. A discontinuous transition is evident in both cases.

Critical couplings for the first-order transition line were determined from the intersection of the energies of the respective phases [Figs. 4(a) and 4(c)]. The second-order transition line was determined from the vanishing of the BAF order parameter (obtained by full-update optimization and extrapolation). We find that the phase diagram, shown in Fig. 1, possesses a first-order transition, out of the DTAF phase, for all values of $J_\times/J_\parallel$. The line of continuous BAF-to-DS transitions extends from the UFB transition to the point $J_\perp = 1.638(15)J_\parallel$, $J_\times = 0.520(5)J_\parallel$, where it terminates on the first-order line. By the definition of Refs. [2,4], this is a QCEP—a CEP occurring at $T = 0$. The term QCEP has been applied by some authors to field-induced magnetic transitions in heavy-fermion systems, apparently to describe critical-point physics (termination of a first-order line) [56], but not in all discussions of the same topic [57].

To our knowledge, there has been very little discussion of the QCEP. In studies of the CEP [4], it is proposed that the critical properties of the terminating line should be reflected in the properties of the discontinuities on the first-order line in the vicinity of the CEP. Unfortunately, we are not presently able to perform finite-T calculations in the vicinity of the QCEP [34]. However, from calculations of ρ_s, of the type shown in Figs. 4(b) and 4(d), we are able to deduce the size of the discontinuity, $\Delta\rho_s$, along the first-order line at $T = 0$ [Fig. 4(e)]. Because ρ_s is related to the energy density, no jump is expected in $\Delta\rho_s$ on passing through the QCEP, due to the continuous nature of the BAF-DS transition. While $\Delta\rho_s$ is indeed continuous within our error bars, our data do suggest a discontinuity in its slope across the QCEP. Certainly the critical properties around the QCEP pose a challenge to presently available numerical methods.

The limit of weak $J_\perp$ and $J_\times$ is of special interest in the frustrated ladder, where the DT-to-DS transition may become continuous [58] and there have been proposals [59] of an intermediate phase. In the frustrated bilayer, our calculations show that the first-order nature of the transition is robust, with finite jumps in the singlet density [Fig. 4(e)] all the way to $J_\perp = J_\times = 0$. The value of $\Delta\rho_s$ in this limit can be understood from the convergence of ρ_s to $1/4$ as $J_\perp \to 0$ in the UFB, where the two layers of the BAF become uncorrelated, but the immediate vanishing of ρ_s when any finite $J_\times$ at $J_\perp = 0$ stabilizes the triplet state. We conclude that the 2D system remains more conventional in this regard than the 1D case.

Returning now to the finite-T Ising critical point, we expect this to persist all the way across the phase diagram of Fig. 1 because of its association with the first-order transition. For confirmation, we perform QMC simulations at $J_\times = 0.7J_\parallel$, where the sign problem remains moderate. As shown in Sec. S1 of the Supplemental Material [34], our results establish that the critical point is still present, occurring at $T = 0.45(1)J_\parallel$. While we are unable by QMC

simulations to study the first-order DTAF-to-BAF transition line, our iPEPS calculations of ρ_s indicate that the binary character of the dimer spin is preserved. We stress that the physics of this line of critical points is a consequence not only of the first-order line but also of the Ising degree of freedom arising due to the dimer-based unit cell.

In summary, we have shown that the frustrated $S = 1/2$ bilayer with only Heisenberg interactions possesses a line of finite-temperature critical points related to a line of first-order transitions in its zero-temperature phase diagram. A second line, of continuous transitions from the rung-singlet to the bilayer-ordered phase, terminates on the first line, creating a QCEP. Understanding the critical properties around the QCEP sets a challenge for theory and numerics both in 2D and in higher dimensions.

This work was supported by the Deutsche Forschungsgemeinschaft (DFG) in the framework of Grants FOR 1807 and RTG 1995, the Swiss National Science Foundation (SNF), and the European Research Council (ERC) under the EU Horizon 2020 research and innovation program (Grant No. 677061). We thank the IT Center at RWTH Aachen University and the JSC Jülich for access to computing time through JARA-HPC.

[1] C. C. de la Tour, Ann. Chim. Phys. **21**, 127 (1822).
[2] P. M. Chaikin and T. C. Lubensky, *Principles of Condensed Matter Physics* (Cambridge University Press, Cambridge, England, 1995), p. 665.
[3] M. E. Fisher and P. J. Upton, Phys. Rev. Lett. **65**, 2402 (1990).
[4] M. E. Fisher and M. C. Barbosa, Phys. Rev. B **43**, 11177 (1991).
[5] S. Sachdev, *Quantum Phase Transitions* (Cambridge University Press, Cambridge, England, 2011).
[6] C. Rüegg, B. Normand, M. Matsumoto, A. Furrer, D. F. McMorrow, K. W. Krämer, H.-U. Güdel, S. N. Gvasaliya, H. Mutka, and M. Boehm, Phys. Rev. Lett. **100**, 205701 (2008).
[7] T. Giamarchi, C. Rüegg, and O. Tchernyshyov, Nat. Phys. **4**, 198 (2008), and references therein.
[8] B. Thielemann, C. Rüegg, H. M. Rønnow, A. M. Läuchli, J.-S. Caux, B. Normand, D. Biner, K. W. Krämer, H.-U. Güdel, J. Stahn, K. Habicht, K. Kiefer, M. Boehm, D. F. McMorrow, and J. Mesot, Phys. Rev. Lett. **102**, 107204 (2009).
[9] R. Yu, L. Yin, N. S. Sullivan, J. S. Xia, C. Huan, A. Paduan-Filho, N. F. Oliveira Jr., S. Haas, A. Steppke, C. F. Miclea, F. Weickert, R. Movshovich, E.-D. Mun, B. L. Scott, V. S. Zapf, and T. Roscilde, Nature (London) **489**, 379 (2012).
[10] P. Merchant, B. Normand, K. W. Krämer, M. Boehm, D. F. McMorrow, and C. Rüegg, Nat. Phys. **10**, 373 (2014).
[11] C. K. Majumdar and D. Ghosh, J. Math. Phys. **10**, 1388 (1969).
[12] B. S. Shastry and B. Sutherland, Physica (Amsterdam) **108B+C**, 1069 (1981).
[13] A. Honecker, S. Wessel, R. Kerkdyk, T. Pruschke, F. Mila, and B. Normand, Phys. Rev. B **93**, 054408 (2016).
[14] A. Honecker, F. Mila, and B. Normand, Phys. Rev. B **94**, 094402 (2016).
[15] L. Savary and L. Balents, Rep. Prog. Phys. **80**, 016502 (2017).
[16] J. Romhányi, K. Penc, and R. Ganesh, Nat. Commun. **6**, 6805 (2015).
[17] S. Wessel, B. Normand, F. Mila, and A. Honecker, SciPost Phys. **3**, 005 (2017).
[18] Y. Xian, Phys. Rev. B **52**, 12485 (1995).
[19] A. Honecker, F. Mila, and M. Troyer, Eur. Phys. J. B **15**, 227 (2000).
[20] M. P. Gelfand, Phys. Rev. B **43**, 8644 (1991).
[21] E. Müller-Hartmann, R. R. P. Singh, C. Knetter, and G. S. Uhrig, Phys. Rev. Lett. **84**, 1808 (2000).
[22] H. Q. Lin and J. L. Shen, J. Phys. Soc. Jpn. **69**, 878 (2000).
[23] H. Q. Lin, J. L. Shen, and H. Y. Shik, Phys. Rev. B **66**, 184402 (2002).
[24] J. Richter, O. Derzhko, and T. Krokhmalskii, Phys. Rev. B **74**, 144430 (2006).
[25] O. Derzhko, J. Richter, A. Honecker, and H.-J. Schmidt, Low Temp. Phys. **33**, 745 (2007).
[26] O. Derzhko, T. Krokhmalskii, and J. Richter, Phys. Rev. B **82**, 214412 (2010).
[27] H. Tanaka, N. Kurita, M. Okada, E. Kunihiro, Y. Shirata, K. Fujii, H. Uekusa, A. Matsuo, K. Kindo, and H. Nojiri, J. Phys. Soc. Jpn. **83**, 103701 (2014).
[28] J. Richter, O. Krupnitska, V. Baliha, T. Krokhmalskii, and O. Derzhko, Phys. Rev. B **97**, 024405 (2018).
[29] A. W. Sandvik, Phys. Rev. B **59**, R14157 (1999).
[30] O. F. Syljuåsen and A. W. Sandvik, Phys. Rev. E **66**, 046701 (2002).
[31] F. Alet, S. Wessel, and M. Troyer, Phys. Rev. E **71**, 036706 (2005).
[32] F. Alet, K. Damle, and S. Pujari, Phys. Rev. Lett. **117**, 197203 (2016).
[33] K.-K. Ng and M.-F. Yang, Phys. Rev. B **95**, 064431 (2017).
[34] See Supplemental Material at http://link.aps.org/supplemental/10.1103/PhysRevLett.121.127201, which contains Refs. [35–40], for details on the QMC sign problem, the finite temperature transition line of the FFB model, and the iPEPS calculations.
[35] D. C. Johnston, R. J. McQueeney, B. Lake, A. Honecker, M. E. Zhitomirsky, R. Nath, Y. Furukawa, V. P. Antropov, and Y. Singh, Phys. Rev. B **84**, 094445 (2011).
[36] P. Corboz, T. M. Rice, and M. Troyer, Phys. Rev. Lett. **113**, 046402 (2014).
[37] T. Nishino and K. Okunishi, J. Phys. Soc. Jpn. **65**, 891 (1996).
[38] R. Orús and G. Vidal, Phys. Rev. B **80**, 094403 (2009).
[39] S. Singh, R. N. C. Pfeifer, and G. Vidal, Phys. Rev. B **83**, 115125 (2011).
[40] B. Bauer, P. Corboz, R. Orús, and M. Troyer, Phys. Rev. B **83**, 125106 (2011).
[41] L. Onsager, Phys. Rev. **65**, 117 (1944).
[42] D. P. Landau, Phys. Rev. B **13**, 2997 (1976).
[43] M. E. Fisher and R. J. Burford, Phys. Rev. **156**, 583 (1967).
[44] K. Hida, J. Phys. Soc. Jpn. **61**, 1013 (1992).
[45] A. J. Millis and H. Monien, Phys. Rev. Lett. **70**, 2810 (1993).
[46] A. W. Sandvik and D. J. Scalapino, Phys. Rev. Lett. **72**, 2777 (1994).

[47] T. Sommer, M. Vojta, and K. W. Becker, Eur. Phys. J. B **23**, 329 (2001).
[48] L. Wang, K. S. D. Beach, and A. W. Sandvik, Phys. Rev. B **73**, 014431 (2006).
[49] F. Verstraete and J. I. Cirac, arXiv:cond-mat/0407066.
[50] Y. Nishio, N. Maeshima, A. Gendiar, and T. Nishino, arXiv:cond-mat/0401115.
[51] J. Jordan, R. Orús, G. Vidal, F. Verstraete, and J. I. Cirac, Phys. Rev. Lett. **101**, 250602 (2008).
[52] G. Vidal, Phys. Rev. Lett. **91**, 147902 (2003).
[53] H. C. Jiang, Z. Y. Weng, and T. Xiang, Phys. Rev. Lett. **101**, 090603 (2008).
[54] H. N. Phien, J. A. Bengua, H. D. Tuan, P. Corboz, and R. Orús, Phys. Rev. B **92**, 035142 (2015).
[55] P. Corboz and F. Mila, Phys. Rev. B **87**, 115144 (2013).
[56] S. A. Grigera, R. S. Perry, A. J. Schofield, M. Chiao, S. R. Julian, G. G. Lonzarich, S. I. Ikeda, Y. Maeno, A. J. Millis, and A. P. Mackenzie, Science **294**, 329 (2001).
[57] D. Belitz, T. R. Kirkpatrick, and J. Rollbühler, Phys. Rev. Lett. **94**, 247205 (2005).
[58] T. Hikihara and O. A. Starykh, Phys. Rev. B **81**, 064432 (2010).
[59] O. A. Starykh and L. Balents, Phys. Rev. Lett. **93**, 127202 (2004).